Optical bandgap of single- and multi-layered amorphous germanium ultra-thin films

Pei Liu,[1] Paolo Longo,[2] Alexander Zaslavsky,[1] and Domenico Pacifici[3,a)]
[1]*Department of Physics and School of Engineering, Brown University, 182-184 Hope St., Providence, Rhode Island 02912, USA*
[2]*Gatan, Inc., 5794 W Las Positas Blvd., Pleasanton, California 94588, USA*
[3]*School of Engineering, Brown University, 184 Hope St., Providence, Rhode Island 02912, USA*

(Received 8 August 2015; accepted 20 December 2015; published online 7 January 2016)

Accurate optical methods are required to determine the energy bandgap of amorphous semiconductors and elucidate the role of quantum confinement in nanometer-scale, ultra-thin absorbing layers. Here, we provide a critical comparison between well-established methods that are generally employed to determine the optical bandgap of thin-film amorphous semiconductors, starting from normal-incidence reflectance and transmittance measurements. First, we demonstrate that a more accurate estimate of the optical bandgap can be achieved by using a multiple-reflection interference model. We show that this model generates more reliable results compared to the widely accepted single-pass absorption method. Second, we compare two most representative methods (Tauc and Cody plots) that are extensively used to determine the optical bandgap of thin-film amorphous semiconductors starting from the extracted absorption coefficient. Analysis of the experimental absorption data acquired for ultra-thin amorphous germanium (a-Ge) layers demonstrates that the Cody model is able to provide a less ambiguous energy bandgap value. Finally, we apply our proposed method to experimentally determine the optical bandgap of a-Ge/SiO_2 superlattices with single and multiple a-Ge layers down to 2 nm thickness. © *2016 AIP Publishing LLC*. [http://dx.doi.org/10.1063/1.4939296]

I. INTRODUCTION

Compared to their crystalline counterparts, the optical properties of amorphous ultra-thin layers are not well understood, even for such mainstream semiconductors as germanium (Ge). Generally, amorphous semiconductors retain short range order and hence can be analyzed within the usual band structure framework, but due to missing long-range order and high defect densities arising from broken bonds, the optical properties are more complex to analyze and model. This complexity increases further in ultra-thin amorphous films, due to quantum confinement effects and high surface state densities.

A widely adopted technique for extracting the optical bandgap of amorphous semiconducting materials was originally proposed by Tauc and co-workers[1] in a seminal paper focusing on bulk a-Ge dating back to 1966. Since then, the Tauc plot has become a standard tool for determining the bandgap of amorphous germanium[2–6] and other materials.[7–13]

Physically, the Tauc model is based on the constant momentum matrix approximation that leads to the following functional dependence $\sqrt{\alpha h\nu} \propto (h\nu - E_g)$, where α is the frequency-dependent absorption coefficient of the material, $h\nu$ is the energy of the incident photon, and E_g is the optical bandgap of the material. E_g can then be determined from the slope and abscissa intercept of a linear fit to the scatter data set.

However, finding an appropriate linear region in the experimental data set can be challenging given the strong energy-dependent slope variation generally observed in the Tauc plot.[14–16] This problem has led Cody and co-workers[14] to propose an alternative model, based on a constant dipole (rather than momentum) matrix approximation, which leads to a different expression for the absorption coefficient as a function of incident photon energy, i.e., $\sqrt{\alpha/h\nu} \propto (h\nu - E_g)$.

Due to the empirical nature and vast variety of current schemes adopted to define the optical bandgap of amorphous semiconductors, practical comparisons and more in-depth discussions of the different approaches are not only useful but also necessary to better understand the applicability constraints of each model. For example, Sweenor *et al*. performed a valuable, detailed study of the relationship between various methods (such as Tauc and Cody plots, among others) to extract the optical bandgap of hydrogenated amorphous silicon.[17]

However, to date, only limited research has been focused on the applicability of either the Tauc or the Cody model to ultra-thin amorphous semiconductor films,[4,6,18–20] even as such films are becoming technologically relevant. For instance, accurate knowledge of the dielectric constants, including the imaginary part of the refractive index that is directly related to the absorption coefficient, can lead to better modeling and design of engineered optical coatings based on ultra-thin amorphous Ge films.[21,22]

In this work, we first quantitatively discuss the simple and popular approach of using a single-path optical model in deriving the absorption coefficient from reflectance and transmittance measurements and show that this approach can lead to ambiguous results in thin (<1000 nm) a-Ge films. Then we demonstrate that the alternative, multiple-reflection

a)Author to whom correspondence should be addressed. Electronic mail: Domenico_Pacifici@brown.edu

interference approach does lead to accurate frequency-dependent absorption coefficient values. Finally, we deduce the optical bandgap of single- and multi-layer (ML) a-Ge films by using both the Cody and Tauc models and compare them in detail. We point out the Tauc fit may produce unreliable optical bandgap values and that the Cody model performs better for ultra-thin films.

II. FABRICATION AND CHARACTERIZATION

Radio frequency (RF) magnetron sputtering was used to deposit a-Ge ultra-thin single- and ML films on various substrates held at room temperature. Specifically, the films were simultaneously deposited both on transparent quartz for optical characterization, and on silicon substrates for structural characterization, such as electron energy loss spectroscopy (EELS) and scanning transmission electron microscopy (STEM) analyses. Because of the amorphous nature of all sputter-deposited layers and thanks to the presence of a native oxide layer on silicon, the samples simultaneously grown on top of the two different substrates are structurally identical.

For single-layer a-Ge films, the Ge film thickness d_{Ge} was varied between 2 and 35 nm. A 10 nm SiO_2 cap layer was deposited on top to avoid ambient contamination and oxidation of the ultra-thin layer. The film thicknesses were calibrated and confirmed through transmission electron microscopy (TEM) measurements.

For the ML a-Ge films, the a-Ge layers were alternated with SiO_2 layers of the same thickness, with the total film thickness fixed at 60 nm (in order to keep the total thickness of both the a-Ge absorbing material and the transparent SiO_2 layers constant at 30 nm) and the individual a-Ge layers varied between 2, 3, 5, and 6 nm. For example, for the 2 nm ML case, the actual configuration was a double layer with $d_{Ge} = 2$ nm and $d_{SiO2} = 2$ nm, repeated 15 times. Two additional ML a-Ge films were also fabricated with $d_{Ge} = 2$ nm/$d_{SiO2} = 1$ nm (15 periods), and $d_{Ge} = 6$ nm/$d_{SiO2} = 1$ nm (5 periods), respectively.

The atomic composition and structural properties of the fabricated samples were quantified by EELS. An example of EELS analysis on a ML sample is shown in Fig. 1. It is seen from the images that the ML sample has good structural properties with generally well-defined transition interfaces between the various layers, and negligible surface roughness, as evidenced by STEM images even for the thinnest samples. The Ge atoms are mostly confined in the wells with very little oxygen contamination present, whereas the SiO_2 oxide barrier layer is shown to be a mixture of SiO and SiO_2, but with SiO_2 being the dominant component. An interface or transition layer between a-Ge and the SiO_2 layer cannot be excluded, but the transition layer width is much less than the SiO_2 barrier width.

Optical characterization of all samples was carried out at room temperature using variable-angle spectroscopic ellipsometry (VASE), as well as reflectance and transmittance measurements at normal incidence, in the 300–1700 nm spectral range, using a calibrated system (QEX10) from PV Measurements, Inc., that was specifically designed to measure specular reflectance.

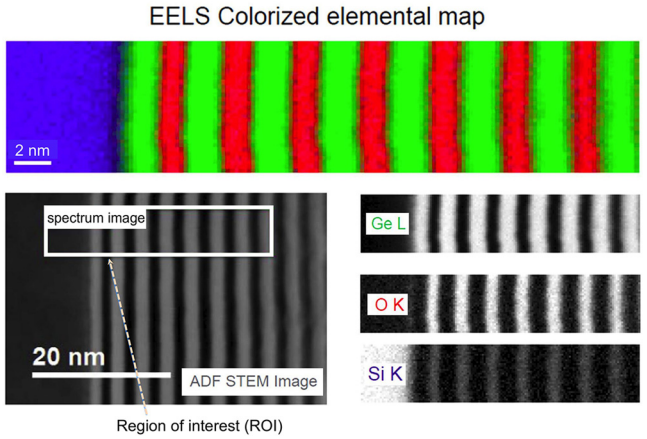

FIG. 1. Electron energy loss spectroscopy (EELS) analysis of a multi-layer (ML) sample consisting of alternating layers of a-Ge and SiO_2 on a silicon substrate. Top panel: EELS colorized elemental map showing Ge atoms in green, O in red, and Si in blue; bottom left panel: scanning transmission electron microscopy (STEM) image of the full ML structure with analysis region of interest marked in the image; bottom right panels: individual EELS elemental maps for Ge (L band), O (K band), and Si (K band).

III. ABSORPTION COEFFICIENT: SINGLE-PASS VS. MULTIPLE INTERFERENCE METHOD

The optical bandgap of a semiconducting material can be determined by extracting the frequency-dependent absorption coefficient from reflectance (R) and transmittance (T) measurements performed at normal incidence. A simple algorithm that is widely used relies on a single-pass approximation that assumes that the incident light beam is exponentially absorbed as it propagates through the film without experiencing thin-film interference effects, thus making it possible to directly use the Beer-Lambert law to derive the absorption coefficient in a straightforward manner.[6,23–26] The key assumption of the Beer-Lambert law is that light intensity in the optically absorbing material decays as $I(x) = I_0 e^{-\alpha x}$, where $I(x)$ is the light intensity after traveling a distance x into the absorbing medium, I_0 is the initial light intensity at $x = 0$, i.e., right inside the absorbing layer, and α is the absorption coefficient. Within this model, the transmittance through a film with thickness d can be expressed as $T = (1-R)e^{-\alpha d}$, where $(1-R)$ is the fraction of the incident light intensity that is not reflected at the first interface and is therefore transmitted into the absorbing layer. Typically, the absorbing layer will be deposited on a thicker substrate which generally has negligible reflection and absorption, such that $T_{sub} \simeq 100\%$. The absorption coefficient α can then be determined from the measured reflectance, R, and transmittance, T, as follows:

$$\alpha(\lambda) = \frac{1}{d} \ln \frac{1 - R(\lambda)}{T(\lambda)}. \quad (1)$$

Although it is generally accepted that the $(1-R)/T$ ratio is able to remove the oscillations in α due to the thin-film interference effects, we will now prove that neglecting

interference effects can significantly invalidate the quantitative analysis of light absorption in thin absorbing films. To illustrate this problem, Fig. 2 presents a series of reflectance and transmittance spectra of a-Ge films in the $d_{Ge} = 10$–500 nm range, simulated using a rigorous multiple-reflection interference model (based on equations discussed below) that uses the complex refractive index determined from ellipsometric measurements on a 35 nm-thick a-Ge film.

To check the validity of the single-pass method, we will use it to extract the absorption coefficients for the different layer thicknesses, applying Eq. (1) to the simulated R and T values as reported in Fig. 2. If the single-pass method is sound, the extracted absorption coefficient curves should be independent of layer thickness, since we are purposely using the same refractive index for all layers, irrespective of their thickness, thus excluding quantum confinement effects that may actually arise in a real thin-film sample.

The results of the analysis are shown in Fig. 3(a), which reports the estimated absorption coefficient curves for various values of film thickness, together with the absorption coefficient calculated directly from the imaginary part of the refractive index, κ (measured via ellipsometry), through the expression $\alpha = 4\pi\kappa/\lambda$.

Although the oscillations originally present in R and T due to multiple interference are suppressed,[10] this cannot be taken as evidence that the extracted values of α are correct. Indeed, Fig. 3(a) demonstrates that significant deviations occur in the extracted absorption coefficients as the film thickness is varied. The single-pass absorption coefficient moves closer to the reference value only for the thicker d_{Ge} (500 nm), although even there some discrepancy at lower energies (i.e., near the relevant band-edge region we wish to characterize) remains. This is to be expected since, for thicker absorbing films, less light is reaching the bottom surface and being reflected, thus bringing the single-pass α values closer to the reference value.

This analysis suggests that the single-pass model can only be trusted for thick films and could lead to significant errors in the estimate of the absorption coefficients for optically thin films, thus potentially affecting the deduced role of quantum confinement effects on the extracted optical bandgaps.

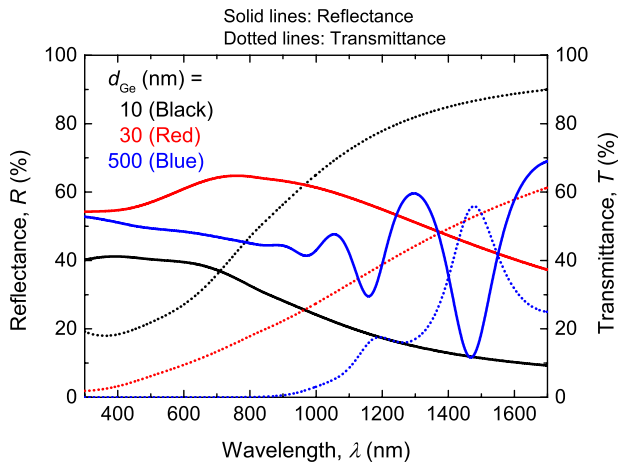

FIG. 2. Simulated reflectance, R (solid lines) and transmittance, T (dashed lines) of a-Ge thin films of different thicknesses. The complex refractive index is taken from variable-angle spectroscopic ellipsometry (VASE) measurements performed on a 35 nm-thick a-Ge film.

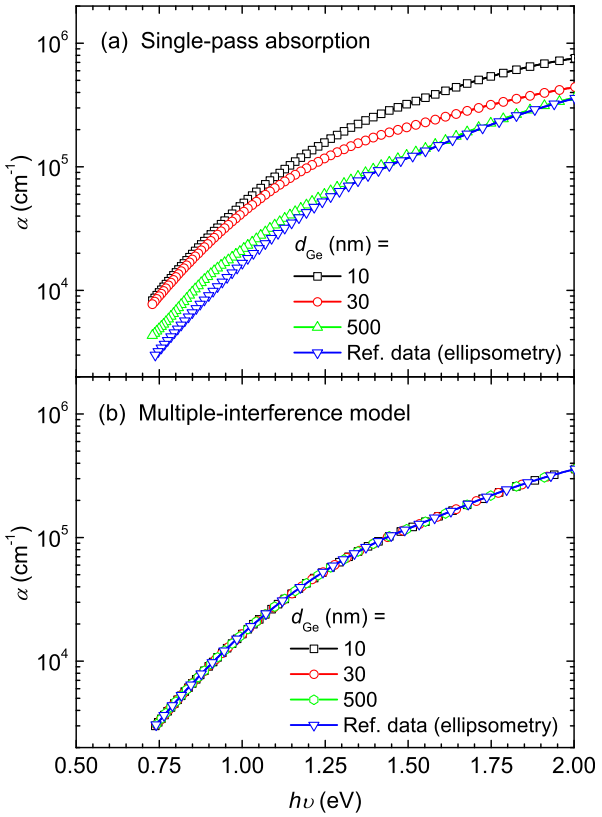

FIG. 3. (a) Absorption coefficients calculated using the single-pass model for different d_{Ge}; (b) absorption coefficients calculated using the multiple interference model (from simulated R and T data as reported in Fig. 2), and reference absorption coefficient calculated from the imaginary part κ of the complex refractive index measured using VASE.

Here, we propose a more accurate method to determine the absorption coefficient from thin-film reflectance and transmittance data by applying a multiple-reflection interference model that uses analytical equations containing Fresnel coefficients and numerical solutions using the transfer matrix method. The calculations are first carried out for normal incidence onto a structure defined by three different refractive indices, i.e., n_1, n_2, and n_3 for the first (generally air), second (the thin film under investigation), and third (the substrate, generally quartz) medium, respectively. The Fresnel reflection coefficient (same for both s and p polarizations under normal incidence) between the interface of medium n_1 and n_2 is

$$r_{12} = \frac{E_r}{E_i} = \frac{n_1 - n_2}{n_1 + n_2}, \tag{2}$$

where E_i is the complex field amplitude of the incident wave and E_r is the complex field amplitude of the wave reflected back into the first medium. The Fresnel transmission coefficient between the interface of medium n_1 and n_2 is

$$t_{12} = \frac{E_t}{E_i} = \frac{2n_1}{n_1 + n_2}, \tag{3}$$

where E_t is the complex field amplitude of waves transmitted into medium n_2. With the above coefficients defined, and including multiple reflections and interference effects, we can write the total reflection and transmission coefficients for a single film as follows:[27]

$$r_{film} = \frac{r_{12} + r_{23}e^{2ik_2d}}{1 + r_{12}r_{23}e^{2ik_2d}}, \tag{4}$$

$$t_{film} = \frac{t_{12}t_{23}e^{ik_2d}}{1 + r_{12}r_{23}e^{2ik_2d}}, \tag{5}$$

where $k_2 = 2\pi n_2/\lambda$ is the wave vector in the film (medium 2) and d is the thickness of the film. Finally, the reflectance and transmittance of the film can be calculated as $R_{theory}(\lambda, d, n, \kappa) = |r_{film}|^2$ and $T_{theory}(\lambda, d, n, \kappa) = |t_{film}|^2$.

In order to extract the spectral dependence of the real, n, and imaginary, κ, parts of the complex refractive index, $n_2 = n + i\kappa$, of the thin film under study, we use the interference model to calculate the reflectance and transmittance of the system (as discussed above) at each wavelength λ and equate them with the measured data (i.e., $R_{data}(\lambda)$ and $T_{data}(\lambda)$)

$$R_{theory}(\lambda, d, n, \kappa) = R_{data}(\lambda), \tag{6}$$

$$T_{theory}(\lambda, d, n, \kappa) = T_{data}(\lambda), \tag{7}$$

where λ and d are all known parameters (d is determined from TEM measurements), and n and κ are the two unknown parameters. Using the bulk reference refractive index data to set the initial guess values for n and κ, the two transcendental equations can be solved numerically. The absorption coefficient can therefore be evaluated from the determined κ as follows:

$$\alpha = \frac{4\pi\kappa}{\lambda}. \tag{8}$$

Figure 3(b) reports the extracted absorption coefficients for all d_{Ge} as extracted from the simulated data $R_{data}(\lambda)$ and $T_{data}(\lambda)$ reported in Fig. 2 after plugging them into Eqs. (6) and (7) and solving them numerically. Evidently, even with different film thicknesses, the extracted absorption coefficients collapse onto a single line that agrees with the original reference data, thus demonstrating the superiority of the multiple interference model compared to the approximate single-pass method.

The importance of an accurate determination of the absorption coefficient for optical bandgap estimation is easily appreciated by constructing standard Tauc plots from the data in Fig. 3. The discrepancy in the absorption coefficients computed from the single-pass model shown in Fig. 3(a) leads to significant uncertainty in the optical bandgaps as obtained from linear fits to the high-energy range of the Tauc plot, as shown in Fig. 4(a). As a result of the varying intercept and slope values, the optical bandgap E_g varies significantly in the 0.7–0.85 eV range, as demonstrated by performing a more detailed analysis shown in Fig. 5. We would like to stress again that quantum confinement effects are purposely not included for the a-Ge layer thicknesses considered in Fig. 5. Therefore, the apparently larger bandgap of the $d_{Ge} = 2$ nm layer is just an artifact introduced by the single-pass method, not an intrinsic property of the material caused by the reduced film thickness. Figure 5 shows a remarkably high (>20%) error in the estimated value of E_g in the relevant range of thicknesses $d_{Ge} =$ 2–300 nm generally used in actual experiments. Even for the

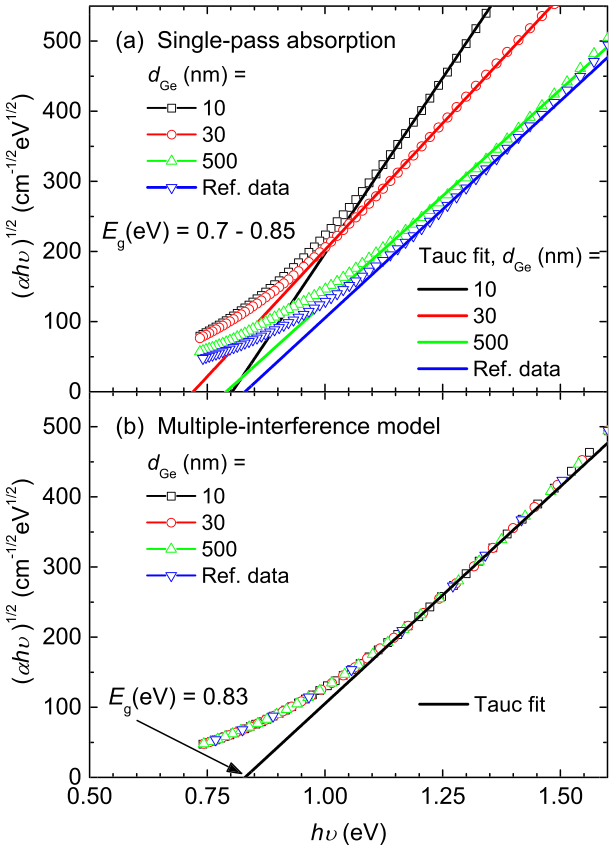

FIG. 4. (a) Tauc plots and fits derived from data in Fig. 3(a); (b) Tauc plots and fits derived from data in Fig. 3(b). Reference data obtained from ellipsometric measurements of the complex refractive index are included for comparison.

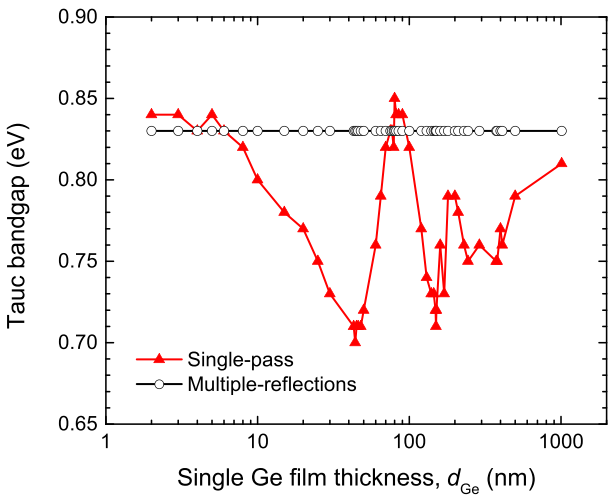

FIG. 5. Optical energy bandgaps determined from linear fits of Tauc plots similar to those reported in Fig. 4, using the single-pass and multiple-reflection interference models, as a function of a-Ge film thickness, d_{Ge}.

thickest $d_{Ge} = 1000$ nm film the Tauc plot obtained from a single-pass method yields an unreliable (although closer) value of energy bandgap compared to the expected, fixed reference value ($E_g = 0.83$ eV) as determined by ellipsometry. Conversely, the multiple-reflection interference approach yields consistent absorption coefficients for all a-Ge film thicknesses (Fig. 3(b)) and, as expected, it is able to produce a unique optical bandgap, as shown in Figs. 4(b) and 5 (open circles). Accordingly, in the remainder of this paper, we will use the multiple-reflection interference model appropriately modified to include an arbitrary number of layers, to estimate the absorption coefficients of various a-Ge/SiO_2 thin-film single- and multi-layers.

Knowledge of the absorption coefficient α by itself is not sufficient to determine the optical bandgap E_g of the amorphous semiconducting layer unless a model exists that relates these two physical quantities. Here, we compare two of the most widely used models, i.e., the Tauc and Cody plots.

It should already be noted that the Tauc plot of Fig. 4(b) is not characterized by a unique slope and hence the determined value of optical bandgap E_g strongly depends on the choice of the linear region. The fit is often performed in an energy range determined by an empirical rule[28] that only considers data points with energy values such that the $\alpha \geq 10^4\,\mathrm{cm}^{-1}$ condition is satisfied. For this reason, the Tauc plot generally leads to higher optical bandgap values compared to the Cody method. Even higher values can be obtained by using another widespread empirical method dubbed the isoabsorption gap, E_{04},[29,30] which defines the optical bandgap as the energy value in the absorption spectrum corresponding to $\alpha = 10^4\ \mathrm{cm}^{-1}$. Due to its arbitrariness, this latter method will not be consider in this paper, although E_{04} can still be easily estimated from the reported absorption graphs. Although the value of the product αd is often used to define the range of photon energies considered to fit the data and extract E_g,[15] this value could be misleading when dealing with thin-film absorbers that may show high absorption due to multiple reflections despite the fact that the material itself is characterized by a small αd value. Moreover, if, as often the case, α is determined using the single-pass model, a large error may be introduced in the actual value of αd, thus making the proposed method less effective in identifying the proper fitting range.

IV. THIN-FILM OPTICAL BANDGAP: EXPERIMENTAL RESULTS AND DISCUSSION

A. Single a-Ge ultra-thin films

For the single a-Ge ultra-thin film samples, we deposited a 10 nm SiO_2 capping layer on top of the Ge film for each sample to prevent ambient contamination. Correspondingly, $R_{theory}(\lambda, d, n, \kappa)$ and $T_{theory}(\lambda, d, n, \kappa)$ are calculated from an extension of the two-layer thin-film system on the quartz substrate based on a straightforward generalization of the multiple-reflection interference model.

Figure 6 reports experimentally measured reflectance, R, transmittance, T, and absorbance, A, spectra as a function of incident photon wavelength, λ, with thickness d_{Ge} of the single a-Ge layer ranging from 2 to 35 nm. From fits of the spectra using Eqs. (6) and (7) with the generalized multiple-reflection interference model, the absorption coefficient α can be determined for all of the thin-film samples.

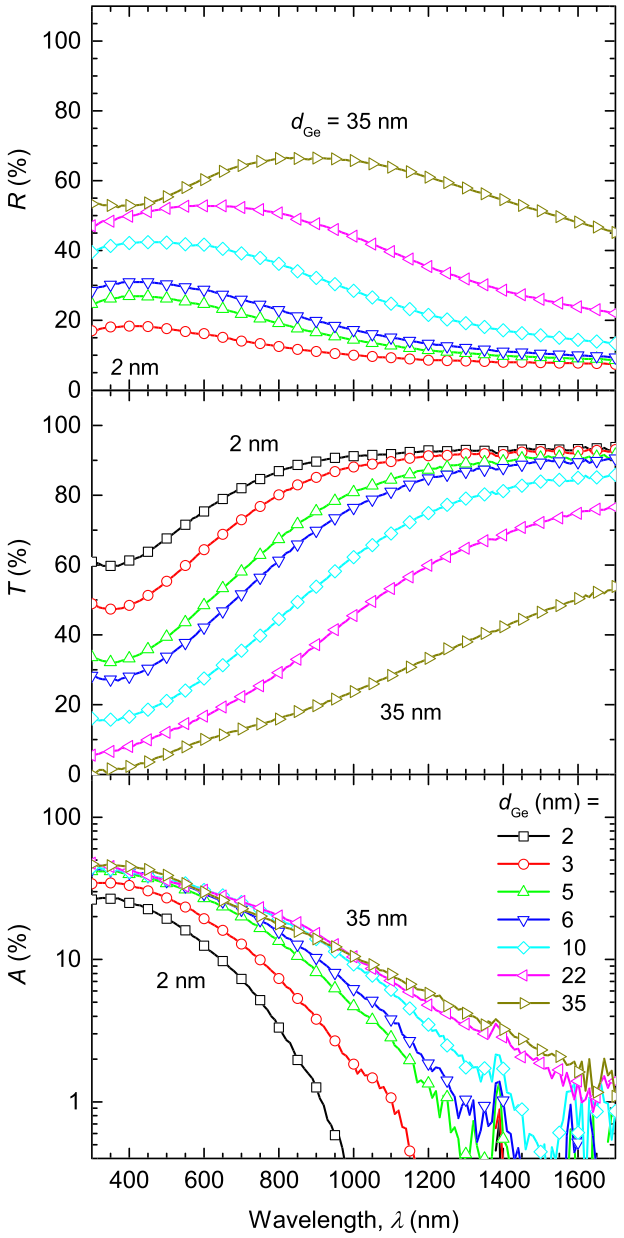

FIG. 6. Experimental reflectance (R), transmittance (T), and absorbance ($A = 1 - R - T$) spectra for individual ultra-thin a-Ge films, at various thicknesses d_{Ge}.

Figure 7 summarizes the derived absorption coefficients of a-Ge ultra-thin films down to $d_{Ge} = 2$ nm. Clearly, the absorption coefficient depends strongly on the film thickness, with a pronounced blue shift for films below 10 nm that can now be ascribed solely to quantum confinement, since potential errors introduced by the single-pass model have been removed. While the overall trend is clear, to quantify the optical bandgaps and discuss the quantum confinement properties, it is necessary to employ the Tauc or Cody model to derive the actual optical bandgap for each case. We first converted the absorption coefficients from Fig. 7 to Tauc plots, by plotting $\sqrt{\alpha h\nu}$ versus $h\nu$.

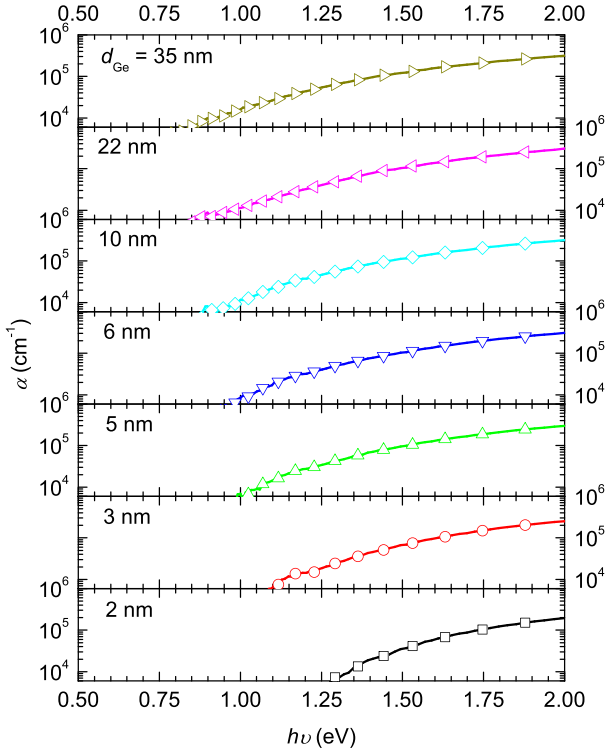

FIG. 7. Absorption coefficients obtained for single a-Ge ultra-thin films at various thicknesses, d_{Ge} (indicated in each panel).

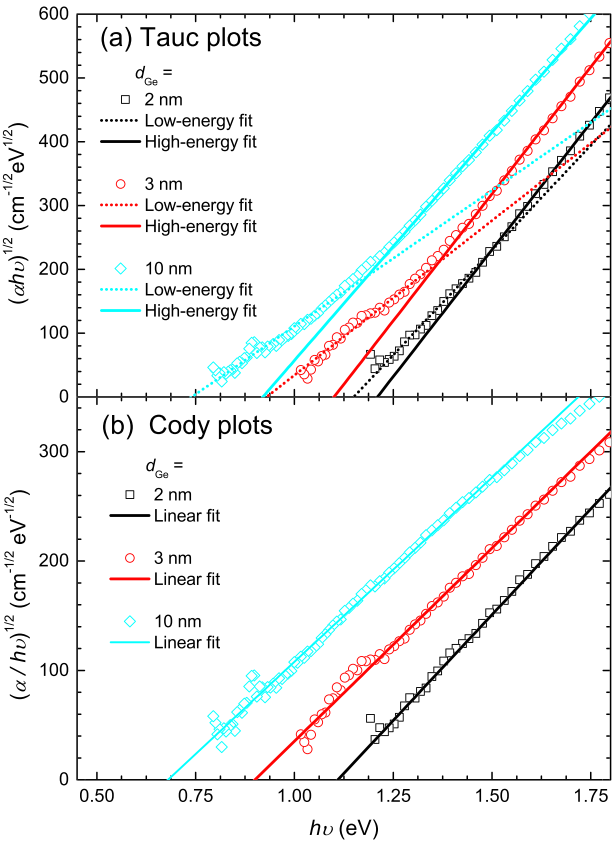

FIG. 8. Representative Tauc (a) and Cody (b) plots and corresponding linear fits for a-Ge ultra-thin single films.

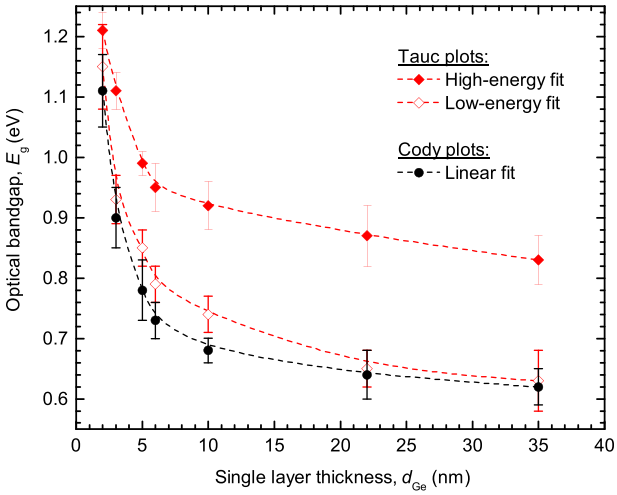

FIG. 9. Optical bandgaps obtained from Tauc and Cody plots via linear fits analogous to those reported in Fig. 8.

In Fig. 8(a), the symbols represent Tauc plots obtained from single films with $d_{Ge} = 2$, 6, and 10 nm. Evidently, Tauc plots generally do not show a single linear trend but rather exhibit a pronounced curvature near the absorption band-edge which greatly affects the bandgap value. Specifically, the linear fits obtained from the high-energy and low-energy regions of each Tauc plot (indicated by solid and dotted lines in Fig. 8(a)) yield markedly different E_g.

For comparison, we also generated Cody plots and fits for the same a-Ge single layer samples in Fig. 8(b), where the symbols represent experimentally measured points and solid lines represent linear fits. Instead of the strong curvature observed in Tauc plots, Cody plots generally show better linear behavior and hence yield an unambiguous value for the optical bandgap.

As a short interim summary of our study of optical bandgaps of single a-Ge ultra-thin films, the optical bandgap values are plotted *vs.* Ge film thickness in Fig. 9 for both Tauc and Cody models. While both models predict a blue shift in the optical bandgap due to size quantization in sufficiently thin a-Ge films, the uncertainty in choosing the energy range for the linear fitting of Tauc plots leads to very large uncertainty in E_g, far larger than the experimental and numerical uncertainty in the Cody model. For this reason, the Cody model appears preferable for the optical bandgap extraction in our samples, a result that may be generally true not only for thick amorphous films (such as hydrogenated amorphous silicon[15]) but also for ultra-thin films of amorphous semiconductors.

Moreover, since curvature effects intrinsic to the Tauc plot method have clearly been demonstrated to induce an apparent increase in the energy bandgap as the film thickness is decreased,[15] the increased linearity in the Cody plots seems to suggest that this method is to be preferred when accurate quantification of quantum confinement effects on the optical bandgap is sought.

B. Multi-layer a-Ge films with thin oxide barriers

In this section, we investigate the optical properties of Ge ML films, consisting of alternating a-Ge/SiO_2 layers with

same thickness, i.e., $d_{Ge} = d_{SiO2}$. The total thickness of the ML is kept constant at 60 nm by changing the number of periods. Accordingly, the integrated thickness of all of the absorbing a-Ge layers in the ML is also kept constant at 30 nm. Therefore, any variation observed in α and E_g as d_{Ge} is decreased can be attributed solely to quantum confinement effects.

Figure 10(a) shows the absorbance spectra A as obtained from experimental reflectance and transmittance data (not shown). Although the total amount of amorphous germanium and the total film thickness of the MLs are kept constant by design, the experimentally measured absorbance spectra show remarkable differences as the individual a-Ge layer thickness is reduced.

In order to better understand the role of quantum confinement on the ML optical properties with different layer configurations, we first took the bulk refractive index of a-Ge from ellipsometric measurements and calculated the optical absorption of all MLs using a classical transfer matrix method. As expected, within the framework of classical effective medium theory, the predicted optical properties of all MLs are identical since the individual layer thicknesses are shorter than all optical wavelengths under consideration. The results shown in Fig. 10(a) as overlapping solid lines demonstrate that all of the MLs are characterized by the same A and α, as expected from a purely classical standpoint.

However, as demonstrated by the experimentally measured absorbance spectra reported in Fig. 10, quantum confinement begins to play an important role when the thickness of each a-Ge film in the ML is reduced below 6 nm.

To further quantify the optical properties of these Ge ML structures, we proceeded again with obtaining the absorption coefficients. As a first approximation, we take the ML film to behave like a single effective layer and calculate the effective absorption coefficient for the whole film, using the previously developed multiple-interference approach. Figure 10(b) shows the resulting absorption coefficients. As the thickness of each Ge layer in the ML is reduced, the absorption coefficient value decreases and the absorption edge shifts to higher energy values, consistent with the direct absorbance measurements in Fig. 10(a). This observation suggests the effective medium theory is still working reasonably well in the quantum regime.

Next, we carried out the Tauc and Cody plot analysis to extract E_g from the absorption coefficient spectra. Figure 11 shows representative Tauc and Cody plots (symbols) and corresponding linear fits (lines) for $d_{Ge} = d_{SiO2} = 2$, 3, and 5 nm ML samples (the $d_{Ge} = d_{SiO2} = 6$ nm case is not shown since it is very close to the 5 nm case). The corresponding optical bandgap values, arising from linear fits of the Tauc and Cody plots, are shown in Figure 12.

Once again, while the determination of the Tauc bandgap is affected by a high variance arising from the

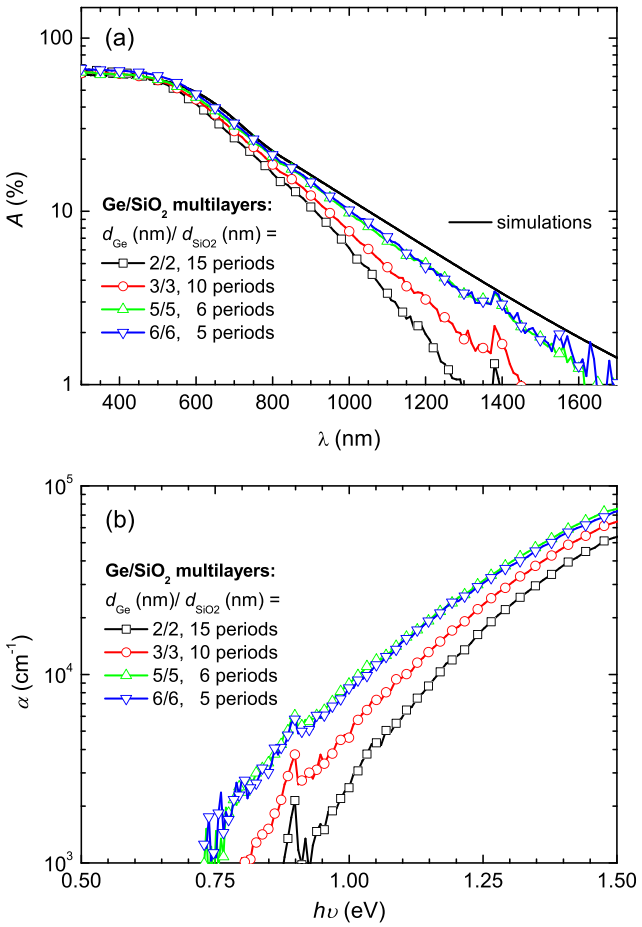

FIG. 10. (a) Absorbance ($A = 1 - R - T$) for a-Ge multi-layer structures as a function of layer thickness: symbols indicate experimentally measured values and solid line represents a classical effective medium calculation (same line for all samples); (b) corresponding absorption coefficients for multi-layer films.

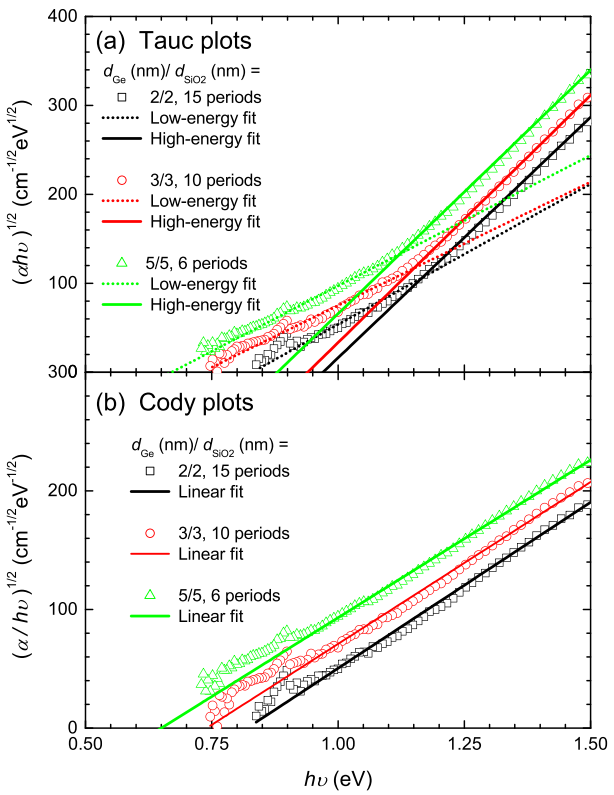

FIG. 11. Representative Tauc (a) and Cody (b) plots and corresponding linear fits for a-Ge multi-layer structures with $d_{Ge} = d_{SiO2} = 2, 3, 5$ nm, respectively.

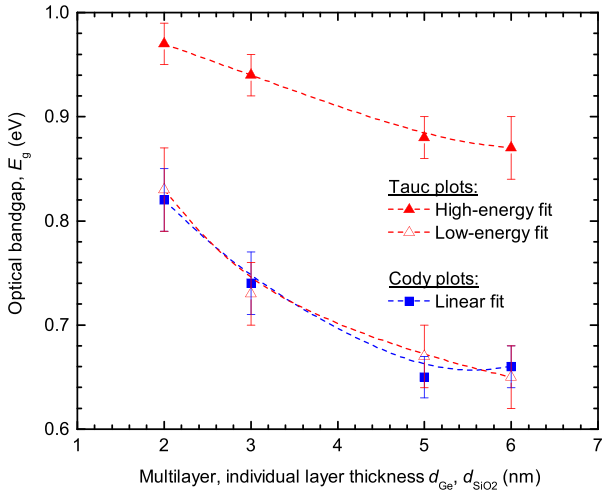

FIG. 12. Optical bandgaps of multi-layer films obtained from Tauc and Cody plots using linear fits analogous to those reported in Fig. 11.

changing slope, the Cody plot method yields a less ambiguous estimate of E_g.

Finally, in Fig. 13, we directly compare the optical Cody-model bandgaps derived from single-layer a-Ge films with their counterparts embedded in ML structures, as a function of layer thickness, d_{Ge}. Interestingly, the optical bandgaps from the different types of structures are not the same, even though the optically absorbing constituent a-Ge layers have the same thickness d_{Ge}. The ML structures (blue squares in Fig. 13) show systematically lower optical gaps compared to their single film counterparts (black circles) and also exhibit a greatly reduced bandgap blue-shift as d_{Ge} is decreased. These observations are consistent with the superlattice-like bandstructure in ML structures, where the thin oxide barriers between the a-Ge layers permit wavefunction overlap between adjacent Ge layers, resulting in overall weaker size quantization.[31] In order to strengthen and further support this interpretation, we fabricated and characterized two additional a-Ge/SiO_2 ML films with a fixed oxide barrier thickness ($d_{SiO2} = 1$ nm) and two different values of $d_{Ge} = 2$ and 6 nm, respectively. The number of periods was chosen to keep the total thickness of a-Ge constant at 30 nm. The optical bandgaps for these two MLs were characterized using the Cody model, following the described method, and the extracted values are reported in Fig. 13 as open triangle and diamond scatter data, respectively. As expected, due to the extremely small oxide layer barrier (1 nm), the MLs effectively behave as a continuous, thicker film of a-Ge, thus displaying the same bandgap value of a reference, thick continuous film.

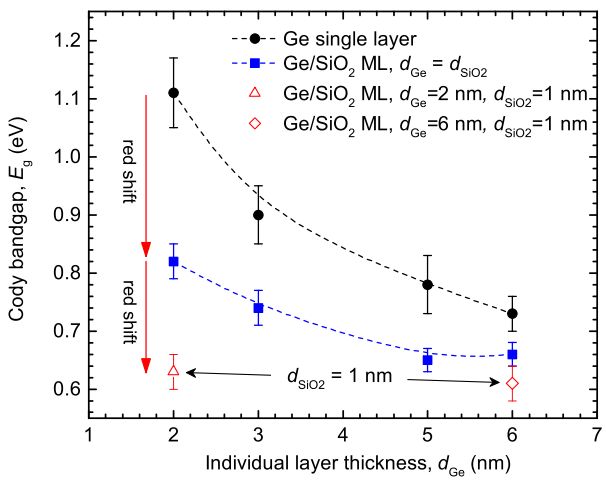

FIG. 13. A comparison between optical bandgaps obtained from the Cody plots for single- and multi-layer a-Ge ultra-thin films.

V. CONCLUSION

We have demonstrated that analysis of reflectance and transmittance spectra using a single-pass optical model can introduce a non-physical thickness dependence on the absorption coefficient of thin dielectric layers. This method, although widely used by the scientific community, can lead to significant errors in estimating the optical bandgap, and therefore strongly impact the analysis of quantum confinement effects. We have shown that a more accurate determination of the absorption coefficient of thin absorbing layers can be achieved by developing a multiple-reflection interference model for the multi-layered system. This model can be used to fit the experimental reflectance and transmittance spectra and determine the real and imaginary parts of the refractive index of the absorbing material, from which the absorption coefficient can be extracted. The optical bandgap of the material can then be determined if the functional dependence of the absorption coefficient *vs.* energy is known. Among several proposed analytical expressions, we have compared the two most-widely used, i.e., the Tauc and Cody plot methods, as representative examples. We have demonstrated with experimental evidence that the Tauc plot can lead to significant uncertainty in the determination of the optical bandgap due to an energy-dependent slope, whereas the Cody model can provide an unambiguous determination of the optical bandgap. The proposed method allows for accurate determination of the optical bandgap of single- and multi-layer a-Ge/SiO_2 superlattices, without requiring empirical assumptions. The proposed approach can be employed to develop improved theoretical models that properly account for quantum confinement effects in ultra-thin absorbing films.

ACKNOWLEDGMENTS

The results and materials presented here are based upon work supported by the National Science Foundation under Grant No. DMR-1203186. The authors would also like to thank D. Li and R. Zia for helpful discussions.

[1]J. Tauc, R. Grigorovici, and A. Vancu, "Optical properties and electronic structure of amorphous germanium," Phys. Status Solidi B **15**, 627 (1966).
[2]L. J. Pilione, K. Vedam, J. E. Yehoda, R. Messier, and P. J. McMarr, "Thickness dependence of optical gap and void fraction for sputtered amorphous germanium," Phys. Rev. B **35**, 9368 (1987).
[3]J. del Pozo and L. Daz, "Thickness dependence of optical gap and absorption tail for amorphous germanium films," Solid State Commun. **87**, 5–8 (1993).
[4]E. S. M. Goh, T. P. Chen, C. Q. Sun, and Y. C. Liu, "Thickness effect on the band gap and optical properties of germanium thin films," J. Appl. Phys. **107**, 024305 (2010).

[5]A. F. Khan, M. Mehmood, A. M. Rana, and T. Muhammad, "Effect of annealing on structural, optical and electrical properties of nanostructured Ge thin films," Appl. Surf. Sci. **256**, 2031–2037 (2010).
[6]S. Cosentino, M. Miritello, I. Crupi, G. Nicotra, F. Simone, C. Spinella, A. Terrasi, and S. Mirabella, "Room-temperature efficient light detection by amorphous Ge quantum wells," Nanoscale Res. Lett. **8**, 128 (2013).
[7]M. H. Brodsky, R. S. Title, K. Weiser, and G. D. Pettit, "Structural, optical, and electrical properties of amorphous silicon films," Phys. Rev. B **1**, 2632 (1970).
[8]H. K. Rockstad, "Hopping conduction and optical properties of amorphous chalcogenide films," J. Non-Cryst. Solids **2**, 192 (1970).
[9]J. M. Essick and R. T. Mather, "Characterization of a bulk semiconductor's band gap via a near-absorption edge optical transmission experiment," Am. J. Phys. **61**, 646–649 (1993).
[10]S. Mirabella, R. Agosta, G. Franzò, I. Crupi, M. Miritello, R. Lo Savio, M. A. Di Stefano, S. Di Marco, F. Simone, and A. Terrasi, "Light absorption in silicon quantum dots embedded in silica," J. Appl. Phys. **106**, 103505 (2009).
[11]M. E. Snchez-Vergara, J. C. Alonso-Huitron, A. Rodriguez-Gmez, and J. N. Reider-Burstin, "Determination of the optical gap in thin films of amorphous dilithium phthalocyanine using the Tauc and Cody models," Molecules **17**, 10000–10013 (2012).
[12]N. A. Kyerematen, V. Hornebecq, H. Martinez, P. Knauth, and T. Djenizian, "Electrochemical fabrication and properties of highly ordered Fe-doped TiO_2 nanotubes," ChemPhysChem **13**, 3707–3713 (2012).
[13]M. Meinert and G. Reiss, "Electronic structure and optical band gap determination of $NiFe_2O_4$," J. Phys.: Condens. Matter **26**, 115503 (2014).
[14]G. D. Cody, B. G. Brooks, and B. Abeles, "Optical absorption above the optical gap of amorphous silicon hydride," Sol. Energy Mater. **8**, 231 (1982).
[15]T. M. Mok and S. K. O'Leary, "The dependence of the Tauc and Cody optical gaps associated with hydrogenated amorphous silicon on the film thickness: Experimental limitations and the impact of curvature in the Tauc and Cody plots," J. Appl. Phys. **102**, 113525 (2007).
[16]R. E. Denton and S. G. Tomlin, "Optical properties of thin germanium films," Aust. J. Phys. **25**, 743 (1972).
[17]D. E. Sweenor, S. K. OLeary, and B. E. Foutz, "On defining the optical gap of an amorphous semiconductor: an empirical calibration for the case of hydrogenated amorphous silicon," Solid State Commun. **110**, 281–286 (1999).
[18]A. Bittar, G. Williams, and H. Trodahl, "Optical absorption and electrical conductivity in amorphous Ge/SiO_x superlattices," Physica A: Stat. Mech. Appl. **157**, 411–417 (1989).
[19]X.-D. Wang, H.-F. Wang, B. Chen, Y.-P. Li, and Y.-Y. Ma, "A model for thickness effect on the band gap of amorphous germanium film," Appl. Phys. Lett. **102**, 202102 (2013).
[20]Y. Abdulraheem, I. Gordon, T. Bearda, H. Meddeb, and J. Poortmans, "Optical bandgap of ultra-thin amorphous silicon films deposited on crystalline silicon by PECVD," AIP Adv. **4**, 057122 (2014).
[21]M. A. Kats, R. Blanchard, P. Genevet, and F. Capasso, "Nanometre optical coatings based on strong interference effects in highly absorbing media," Nat. Mater. **12**, 20–24 (2012).
[22]M. A. Kats and F. Capasso, "Ultra-thin optical interference coatings on rough and flexible substrates," Appl. Phys. Lett. **105**, 131108 (2014).
[23]J. Wang, J. T. Chen, B. B. Miao, F. Zhang, and P. X. Yan, "The effect of hydrogen on Cu_3N thin films deposited by radio frequency magnetron sputtering," J. Appl. Phys. **100**, 103509 (2006).
[24]M. E. Snchez-Vergara, J. R. lvarez Bada, C. O. Perez-Baeza, E. A. Loza-Neri, R. A. Torres-Garca, A. Rodrguez-Gmez, and J. C. Alonso-Huitron, "Morphological and optical properties of dimetallo-phthalocyanine-complex thin films," Adv. Mater. Phys. Chem. **4**, 20–28 (2014).
[25]X. Li, H. Zhu, J. Wei, K. Wang, E. Xu, Z. Li, and D. Wu, "Determination of band gaps of self-assembled carbon nanotube films using Tauc/Davis-Mott model," Appl. Phys. A **97**, 341 (2009).
[26]L. Magafas, "The effect of thermal annealing on the optical properties of a-SiC:H films," J. Non-Cryst. Solids **238**, 158–162 (1998).
[27]O. Heavens, *Optical Properties of Thin Solid Films*, Dover Books on Physics Series (Dover Publications, 1991).
[28]S. Knief and W. von Niessen, "Disorder, defects, and optical absorption in $a-Si$ and $a-Si:H$," Phys. Rev. B **59**, 12940–12946 (1999).
[29]S. K. O'Leary, S. Zukotynski, and J. M. Perz, "Semiclassical density-of-states and optical-absorption analysis of amorphous semiconductors," Phys. Rev. B **51**, 4143–4149 (1995).
[30]S. K. O'Leary, S. Zukotynski, and J. M. Perz, "Optical absorption in amorphous semiconductors," Phys. Rev. B **52**, 7795–7797 (1995).
[31]J. H. Davies, *The Physics of Low-Dimensional Semiconductors* (Cambridge University Press, 1998).